

## *Parvimonas micra*-polarized M2-like tumor-associated macrophages accelerate colorectal cancer development via IL-8 secretion

Dang Khoa Nguyen<sup>a,b,c,\*</sup>, Min-Jung Kang<sup>a\*</sup>, Su-Jeong Oh<sup>a,b,c</sup>, Hee-Jeong Park<sup>a,b,c</sup>, Seong Hui Kim<sup>a,b,c</sup>, Jeong Hyun Yu<sup>a,b,c</sup>, Yunji Lee<sup>a,b,c</sup>, Hyeon Seo Lee<sup>a,b,c</sup>, Ji Won Yang<sup>a</sup>, Yoojin Seo<sup>a</sup>, Ji-Su Ahn<sup>a</sup> and Hyung-Sik Kim<sup>a,b,c</sup>

<sup>a</sup>Department of Oral Biochemistry, Dental and Life Science Institute, School of Dentistry, Pusan National University, Yangsan, Republic of Korea; <sup>b</sup>Department of Life Science in Dentistry, School of Dentistry, Pusan National University, Yangsan, Republic of Korea; <sup>c</sup>Education and Research Team for Life Science on Dentistry, Pusan National University, Yangsan, Republic of Korea

### ABSTRACT

*Parvimonas micra* (*Pm*), a periodontal pathogen, has been implicated in the impairment of anti-tumor responses in colorectal cancer (CRC). The tumor microenvironment in CRC involves tumor-associated macrophages (TAMs), which are pivotal in modulating tumor-associated immune responses. The polarization of TAMs towards an M2-like phenotype promotes CRC progression by suppressing the immune system. However, the mechanisms by which *Pm* affects the progression of CRC remain inadequately elucidated. In this study, we explored the impact of *Pm* infection on CRC cell characteristics, including proliferation, chemoresistance, migration, and macrophage polarization. We found that *Pm*-infected THP-1-derived macrophages exhibited elevated interleukin-10 levels, a well-established M2 marker. Conditioned media from *Pm*-treated THP-1 cells significantly enhanced CRC cell proliferation, cisplatin resistance, and migration, and interleukin-8 was identified as a key factor. Consistent with the *in vitro* results, an azoxymethane/dextran sodium sulfate mouse model treated with oral *Pm* showed accelerated CRC tumor growth. These results offer mechanistic insights into the influence of *Pm* infection on tumor microenvironment in CRC through M2-like macrophage polarization. The identified pathways may serve as potential targets for therapeutic interventions for CRC.

### ARTICLE HISTORY

Received 16 August 2024  
Revised 27 October 2024  
Accepted 29 November 2024

### KEYWORDS

*Parvimonas micra*; host-microbe interaction; colorectal cancer; tumor microenvironment

## 1. Introduction


Periodontitis, a serious form of gum disease, is characterized by the inflammation and infection of the tissue-supporting structures around the teeth (Andriankaja et al. 2023). Its pathogenesis involves microbial attachment and growth on tooth surfaces, which triggers chronic immune responses (Hajishengallis 2015). Several studies have indicated that periodontitis is associated with an increased risk of CRC development and progression (Hou et al. 2022; Idrissi Janati et al. 2022).

CRC has the third highest global prevalence and the fourth highest mortality rate (Rawla et al. 2019) with many patients passing away by the age of 50 years, and its incidence is still gradually rising among young people (Awedew et al. 2022; Stoffel and Murphy 2020). Various factors contribute to CRC progression, including genetic factors, environmental changes, diet, and gut microbiota (Kim and Lee 2021; Nguyen and Duong

2018). Recent evidence suggests a correlation between gut microbiota and CRC development (Fong et al. 2020; Koveitypour et al. 2019; Liu et al. 2023).

Several periodontal pathogens, including *Fusobacterium nucleatum* (*F. nucleatum*), *Porphyromonas gingivalis*, and *Peptostreptococcus anaerobius*, have been linked to CRC progression (Mohammadi et al. 2022). However, the specific roles of these pathogens in CRC development remain unclear.

*F. nucleatum*, a well-studied oral pathogen, is known to promote CRC progression by modulating immune responses and creating a pro-inflammatory tumor microenvironment. *F. nucleatum* interacts with colorectal epithelial and immune cells, facilitating tumorigenesis through mechanisms such as activation of the Toll-like receptor (TLR)4/NF- $\kappa$ B pathway, which promotes M2-like macrophage polarization and suppresses anti-tumor immunity (Guo et al. 2021; Hu et al. 2021). Despite its established role in CRC, it is crucial to study

**CONTACT** Ji-Su Ahn  anjs08@naver.com; Hyung-Sik Kim  hskimcell@pusan.ac.kr  Department of Oral Biochemistry, School of Dentistry, Pusan National University, Yangsan 50612, Republic of Korea

\*These authors contributed equally to this work.

© 2024 The Author(s). Published by Informa UK Limited, trading as Taylor & Francis Group

This is an Open Access article distributed under the terms of the Creative Commons Attribution-NonCommercial License (<http://creativecommons.org/licenses/by-nc/4.0/>), which permits unrestricted non-commercial use, distribution, and reproduction in any medium, provided the original work is properly cited. The terms on which this article has been published allow the posting of the Accepted Manuscript in a repository by the author(s) or with their consent.

other oral pathogens that may operate through distinct mechanisms to promote tumor progression.

*Parvimonas micra* (*Pm*), a gram-positive anaerobic bacterium commonly found in oral diseases, has been reported to have a higher prevalence in CRC patients (Lowenmark et al. 2022; Mohammadi et al. 2022; Osman et al. 2021). Similar to *F. nucleatum*, *Pm* has also been linked to molecular subtype 1 of CRC, which is characterized by immune cell infiltration and activation of specific inflammatory pathways (Lowenmark et al. 2022; Purcell et al. 2017). Given that *F. nucleatum* induces M2-like macrophage polarization, it is plausible that *Pm* could exert similar effects on the tumor microenvironment, facilitating CRC progression. Therefore, we hypothesize that *Pm* may contribute to CRC development by promoting an immunosuppressive microenvironment, similar to *F. nucleatum*.

The tumor microenvironment (TME) is crucial in cancer progression and metastasis, with inflammatory stages significantly affecting CRC (Kim et al. 2024; Lee et al. 2022; Zhao et al. 2022). Tumor-associated macrophages (TAMs) within TME have been linked to adverse outcomes in various cancers (Hourani et al. 2021; Kim et al. 2024). Macrophages in TME can adopt M1-like or M2-like phenotypes. M1-like macrophages mediate pro-inflammatory responses and anti-tumor immunity while M2-like macrophages are associated with tumor growth and metastasis (Biswas and Mantovani 2010; Chen et al. 2023; Perez-Gonzalez et al. 2023). TAMs predominantly display an M2-like phenotype, stimulating tumor progression through immune suppression (Hao et al. 2012). The interaction between TAMs and cancer cells activates epithelial–mesenchymal transition (EMT), leading to increased CRC migration, invasion, and metastasis (Feng et al. 2023; Pan et al. 2021). However, the exact mechanisms linking *Pm* infection, macrophage polarization, and CRC remain unclear.

In this study, we investigated the influence of *Pm* on macrophage polarization and CRC cells, using an azoxymethane/dextran sodium sulfate (AOM/DSS) mouse model with *Pm* gavage. Our results revealed that *Pm*-induced M2-like macrophage polarization significantly elevated pro-inflammatory cytokine IL-8, contributing to CRC progression. Consistent with *in vitro* data, *in vivo* results showed a significant acceleration of tumor growth in CRC. These findings suggest that targeting *Pm*-induced macrophage polarization and interleukin (IL)-8 secretion could enhance CRC immune therapies.

## 2. Materials and methods

### 2.1. Bacterial strain and culture

A strain of *Pm* ATCC 33270 was obtained from the American Type Culture Collection (Manassas, VA, USA). The

*Pm* bacterial strain was cultivated under anaerobic conditions using the BD GasPak™ EZ Anaerobe container system (Becton Dickinson, Canada) at 37°C in Gifu Anaerobic Broth media (Nissu, Tokyo, Japan), supplemented with hemin and vitamin K. *Pm* bacteria were collected by centrifugation at 4°C and 3000 rpm for 10 min, followed by a single wash with PBS. The bacterial suspensions were then resuspended in Roswell Park Memorial Institute medium (RPMI-1640; Gibco, Grand Island, NY, USA), and the optical density was measured at 600 nm, resulting in a concentration of  $1 \times 10^9$  colony-forming unit (CFU)/mL.

### 2.2. Cell culture

All cell lines were obtained from the Korean Cell Bank (Republic of Korea). The human CRC cell lines HT-29 and HCT-116, as well as human monocyte THP-1 cells, were cultured in RPMI-1640 medium, while BV-2 microglial cells and RAW 264.7 were cultured in high-glucose Dulbecco's Modified Eagle Medium (DMEM; Gibco). Both media were supplemented with 10% fetal bovine serum (FBS, Gibco) and 1% penicillin/streptomycin (Gibco). The cell cultures were maintained at 37°C with 5% CO<sub>2</sub> and 95% humidity. For macrophage differentiation,  $1 \times 10^6$  THP-1 cells were seeded in each well of a 6-well plate and treated with 100 ng/mL phorbol myristate acetate (PMA; Sigma, St. Louis, MO, USA) for 24 h. After successful macrophage stimulation, the cells were washed once with PBS and cultured in a fresh medium for subsequent experiments. For mouse macrophage experiments, BV-2 cells ( $4 \times 10^5$  cells/well) and RAW 264.7 cells ( $1 \times 10^6$  cells/well) were seeded into each well of a 6-well plate and incubated for 24 h. Following attachment, the cells were washed with PBS and supplemented with fresh high-glucose DMEM containing 1% FBS. These cells were used for subsequent experiments.

### 2.3. Conditioned media preparation of *Pm*-treated THP-1 cells

THP-1 macrophages in 6-well plates were washed with PBS and replenished with fresh RPMI-1640 medium containing 10% FBS. THP-1 were then treated with PMA (100 ng/mL) for 24 h. After stabilization, *Pm* were infected at a multiplicity of infection (MOI) of 200 for 24 h. The supernatant was collected and clarified using a 0.22- $\mu$ m filter (Jet biofilm, FBE, Guangzhou, China) to eliminate the bacteria and cellular debris before storage in a –80°C refrigerator for subsequent analysis. Finally, the supernatant was combined with fresh RPMI-1640 medium, containing 10% FBS in a 1:2 ratio,

to create CM of macrophages and macrophages *Pm*-treated (CM-*Pm*).

#### 2.4. Cell proliferation and cisplatin resistance assay

To evaluate the proliferation of CRC cells, the Cell Counting Kit-8 (CCK-8; Dojindo, Kumamoto, Japan) was used according to the manufacturer's guidelines. HT-29 and HCT-116 cells were plated in 96-well plates and incubated at 37°C in 5% CO<sub>2</sub> for 24 hours. For *Pm* treatment, cells were infected with *Pm* at MOIs of 100 and 200. In the CM experiments, the cell culture medium was replaced with CM, CM-*Pm*, or fresh medium (control). After 24, 48, and 72 h of co-culture, 10 µL of CCK-8 reagent was added, followed by incubation at 37°C for 1 h. The absorbance was measured at 450 nm to calculate cell proliferation. For analysis of cisplatin resistance, cells were plated in a 96-well plate with the same cell numbers as in proliferation analysis and incubated at 37°C for 24 h. *Pm* was infected at MOIs of 100 and 200 or CM and CM-*Pm* were added to the cells. Subsequently, cisplatin (0, 3.75, 7.5, 15, and 30 mM) was added simultaneously with *Pm* treatment or CM and incubated for 48 h. After incubation, CCK-8-reagent was added to each well, and absorbance values were measured at 450 nm to calculate the cell viability.

#### 2.5. Wound healing assay

HT-29 (2 × 10<sup>5</sup> cells/well) and HCT-116 (1 × 10<sup>5</sup> cells/well) were separately seeded in 6-well culture plates and incubated at 37°C until they reached approximately 80-90% confluence. In each well, two wound lines were created by gently scraping the cell surface with a sterile 200 µL plastic pipette tip. The remaining cells were then washed with PBS to remove cellular debris. For *Pm* infection, wounded cells were supplied with RPMI-1640 medium containing 10% FBS and subsequently infected with *Pm* at MOIs of 100 and 200. For conditioned media, CM and CM-*Pm* were prepared as previously mentioned, added to the cells, and incubated at 37°C. Wound behavior was monitored using microscopy, and images were captured immediately after creating the wound (0 h) and at 24 and 48 h. Five images of each wound area were taken. The average wound area (%) was quantified using the ImageJ Software (National Institutes of Health, Bethesda, Maryland, USA).

#### 2.6. ELISA

Supernatants from untreated and *Pm*-treated macrophages were collected and centrifuged at 300 RCF for

5 min. The supernatants of THP-1 and RAW 264.7 cells were harvested after 24 h of *Pm* infection, while the BV-2 supernatant was collected after 48 h. These samples were preserved at 80°C for future ELISA analysis. Commercial kits obtained from R&D Systems (Abingdon Science Park, UK) were used to measure the concentrations of IL-10 and IL-8 according to the manufacturer's instructions.

#### 2.7. RNA extraction and RT-PCR

Total mRNA from THP-1 cells treated with *Pm* and colon tissues was extracted using the Pury RNA Plus Kit (GenDEPOT, Baker, TX, USA) following the manufacturer's instructions. Subsequently, cDNA was synthesized from 1 µg of total RNA using ReverTra Ace® PCR RT Master Mix (Toyobo, Osaka, Japan). qPCR was performed on an ABI 7500 real-time PCR device (Applied Biosystems, Carlsbad, CA, USA) using the SYBR Green PCR Master Mix (Thermo Scientific, Waltham, MA, USA) and specific primers. The C<sub>t</sub> value of the housekeeping gene *GAPDH* was used to normalize the gene expression levels. The primer sequences used were: Human *GAPDH* Forward 5'-GTCTCTGACTTCAACAGCG-3', Reverse 5'-ACCACCCTGTTGCTGTAGCCAA-3'; Human IL-10 Forward 5'-CAAGACCCAGACATCAAGGCG-3', Reverse 5'-GCATTCTTACCTGCTCCACG-3'; Human CD-206 Forward 5'-GTCATATCGGGTTGAGCCACT-3', Reverse 5'-AATCATTCCGTTACCAGAGG-3'; Human IL-8 Forward 5'-AAACCACCGGAAGGAACCAT-3', Reverse 5'-CCTTCACACAGAGCTGCAGAAA-3'; Human TGF-β Forward 5'-CTTTCCTGCTTCTCATGGCC-3', Reverse 5'-TCCAGGCTCCAAATGTAGGG-3'; Human CCL-2 Forward 5'-AAGATCTCAGTGCAGAGGCTCG-3', Reverse 5'-CACAGATCTCCTTGCCACAA-3'; Human IL-6 Forward 5'-AATAACCACCCCTGACCCAAC-3', Reverse 5'-ACATTTGCCGAAGAGCCCT-3'; Human IL-1β Forward 5'-TGAAGTCAAAGCTCTCCACC-3', Reverse 5'-CTGATGTACCAGTTGGGGAA-3'; Human CCL-18 Forward 5'-AGATCTGTGCTGACCCCAAT-3', Reverse 5'-TGAAGAGGACCTGGGAGTAG-3'; Mouse *GAPDH* Forward 5'-GGAAGGGCTCATGACCAC-3', Reverse 5'-GCAGGGATGATGTTCTGG-3'; Mouse CD-206 Forward 5'-GCCTGATGCCAGGTTAAAGCA-3', Reverse 5'-GAGGGAAGCGAGAGATTATGGA-3'; Mouse IL-8 Forward 5'-ATGGCTGCTCAAGGCTGGT-3', Reverse 5'-AGGCTTTTCATGCTCAACACTAT-3';

#### 2.8. Transwell migration assay

To analyze the migratory ability of CRC cells, a 24-well Transwell cell culture chamber with an 8.0-µm pore size (SPL Life Sciences, Gyeonggi-do, Korea) was used. A total of 1 × 10<sup>5</sup> cells per well (HT-29 and HCT-116)

were seeded in 6-well plates and left to attach for 24 h. After incubation, cells were treated with CM and CM-*Pm* for 48 h. Subsequently,  $2 \times 10^4$  cells were resuspended in 200  $\mu$ L of RPMI-1640 medium containing 10% FBS and placed in the upper inserts, while 400  $\mu$ L of RPMI medium supplemented with 10% FBS was added in the lower chamber. Following 24 h of incubation, the medium in the upper insert was exchanged with 200  $\mu$ L RPMI medium without FBS, while the medium in the lower chamber medium was replenished with 20% FBS. After an additional 24 h of incubation, cells on the membrane were removed using cotton swabs. The cells that migrated to the lower surface of the membrane were fixed with 100% ethanol for 10 min and stained with 0.5% crystal violet for 20 min. Subsequently, the cells were washed four times with PBS for 5 minutes each. Finally, cells in five microscopic fields at 40 $\times$  magnification were observed, photographed, and counted using the ImageJ Software.

### 2.9. AOM/DSS colorectal carcinogenesis model

All experiments were approved by and conducted in accordance with the regulations of the Pusan National University Institutional Animal Care and Use Committee (IACUC, No. 2022-034-A1C0). The mice were housed in a controlled environment with a 12-hour light/dark cycle, temperature of  $22 \pm 2^\circ\text{C}$ , and humidity of  $55 \pm 5\%$ . Standard rodent chow and water were provided ad libitum. Environmental enrichment, such as nesting material, was provided to promote animal welfare. To minimize suffering, all animals were monitored daily for signs of discomfort, illness, or abnormal behavior. Sample size was determined based on previous studies and the expected effect size of the treatments. Humane endpoints were established to minimize suffering. Eight-week-old male C57BL/6 mice were divided into three groups: an AOM/DSS + *Pm* group, an AOM/DSS + PBS group (each group contained 12 mice), and a control group with five mice. Mice were intraperitoneally injected with 10 mg of AOM (Sigma) per kg body weight. Starting with the AOM injection, mice were orally gavaged with *Pm* at a dosage of  $1 \times 10^9$  CFU or PBS three times a week throughout the experiment. After five days, 2% DSS (MP Biomedicals, Solon, OH, USA) was added to the drinking water for five days, followed by a return to regular drinking water for two weeks. This cycle was repeated twice, and the mice were euthanized on day 70. Colon tissues were carefully removed surgically and collected for further examination. This study complied with the ARRIVE 2.0 guidelines for reporting animal research.

### 2.10. Statistics analysis

All results were analyzed using GraphPad Prism software (version 10.0, San Diego, CA, USA). Statistical evaluation was conducted using a two-tailed Student's t-test and one-way or two-way analysis of variance (ANOVA), followed by the Bonferroni post hoc test for multi-group comparison. Data are presented as mean  $\pm$  standard deviation (SD). Significance was defined as  $*P < 0.05$ ,  $**P < 0.01$ ,  $***P < 0.001$ , and  $****P < 0.0001$ .

## 3. Results

### 3.1. Effects of *Pm* on the characteristics of CRC cells

To investigate the cellular responses of CRC to *Pm*, we initially examined the proliferation of CRC cells upon *Pm* infection. Two CRC epithelial cell lines, HT-29 and HCT-116, were infected with *Pm* for 72 h. The *Pm* infection led to a slight increase in the proliferation of CRC (Figure 1(A)). To further understand the impact of *Pm* infection on chemotherapeutic responses of CRC cells, they were exposed to various concentrations of cisplatin in the presence and absence of *Pm*. Both HT-29 and HCT-116 cells demonstrated a dose-dependent decrease in growth following cisplatin treatment, showing marginally increased viability due to *Pm* infection (Figure 1(B)). Additionally, we conducted wound healing assays to evaluate the migratory activity of CRC cells upon *Pm* infection. The results showed that *Pm* infection at a MOI of 200 significantly enhanced the migration of HT-29 cells, but a similar effect was not observed in HCT-116 cells (Figure 1(C)–(F)). However, compared to the control, CRC cells infected with *Pm* exhibited faster wound closure (Figure 1(C)–(F)). These results suggest that *Pm* slightly enhances the proliferative, cisplatin-resistant, and migratory characteristics of CRC cells.

### 3.2. *Pm* induces M2-like polarization of macrophages

It has been reported that the representative oral pathogen *F. nucleatum* induces the M2-like polarization of macrophages, a phenomenon that is often correlated with CRC progression (Hu et al. 2021; C. Xu et al., 2021). Therefore, we investigated whether *Pm* can also induce similar phenotypic changes in macrophages. THP-1 macrophages were treated with *Pm*, and the supernatants were collected for ELISA. A significantly elevated level of IL-10, a representative M2 cytokine, was observed in the supernatants of THP-1 treated

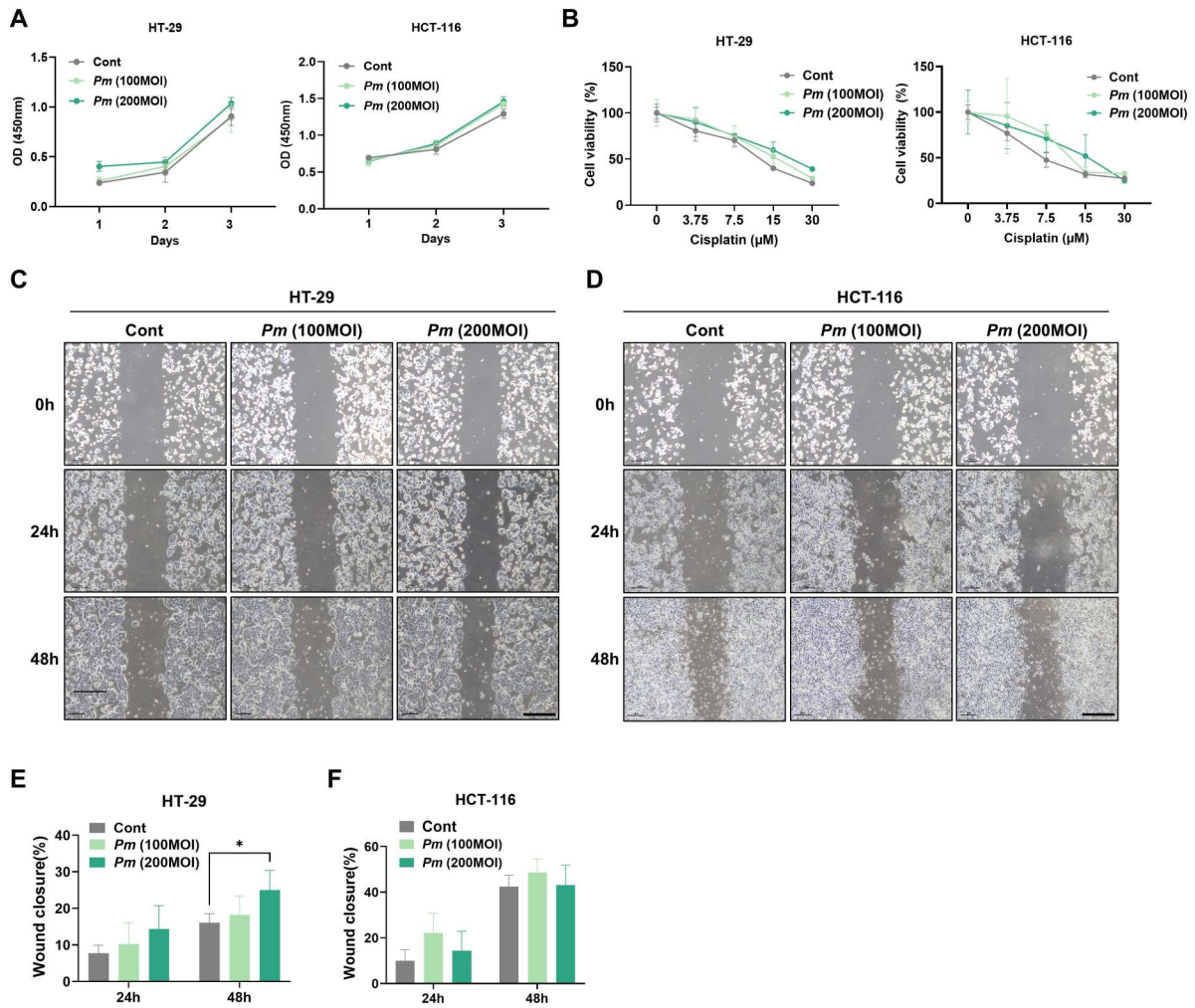


**Figure 1. *Pm* affects the characteristics of CRC cells and participates in the M2-like polarization of macrophages.** (A) CCK8 assay was performed to evaluate the proliferation capability of CRC cells (HT-29 and HCT-116) co-cultured with *Pm* (MOIs of 100 and 200) for 24, 48, and 72 h. (B) Cisplatin resistance was examined in CRC cells co-cultured with *Pm*. (C-F) Wound healing assays were conducted, and wound closures (%) were assessed to measure the mobility of CRC cells co-cultured with *Pm* for 24 and 48 h. Scale bar: 100  $\mu$ m. All data are displayed as the mean  $\pm$  SD. \* $P < 0.05$ .

with *Pm* or IL-4 (as a positive control) compared to the untreated control (Figure 2(A)). Notably, the concentration of IL-10 was noticeably increased in the *Pm*-treated sample at an MOI of 200. These findings suggest that *Pm* participates in the M2-like polarization of macrophages. To further confirm the involvement of *Pm* in the M2-like polarization of macrophages, the expression of CD-206 in *Pm*-infected THP-1 was measured using flow cytometric analysis. *Pm* infection significantly increased the number of CD206-positive cells at a MOI of 200, compared to both the MOI of 100 and the untreated control (Figure 2(B)). Additionally, qRT-PCR analysis revealed elevated mRNA levels of IL-10 and CD-206 in THP-1 cells infected with *Pm* (Figure 2(C), (D)). To determine whether similar results could be observed in mouse macrophages, the macrophage cell line Raw-264.7 and the microglia cell line BV-2 were

infected with *Pm*. Upon *Pm* infection, IL-10 production from these cells was also elevated, indicating M2 polarization (Figure 2(E), (F)). These findings further suggest that *Pm* contributes to the M2-like polarization of macrophages.

### 3.3. *Pm*-induced M2-like macrophages deteriorate the tumor characteristics in CRC cells

Immune cells within the TME play a vital role in suppressing or promoting tumorigenesis and cancer progression. Recent research has suggested that oral bacteria, such as *F. nucleatum*, might inhibit anti-tumor immunity, thus potentially facilitating the CRC (Hu et al. 2021; C. Xu et al., 2021). Therefore, to further investigate the effects of *Pm* on M2-like macrophages in the progression of CRC, we used the conditioned medium

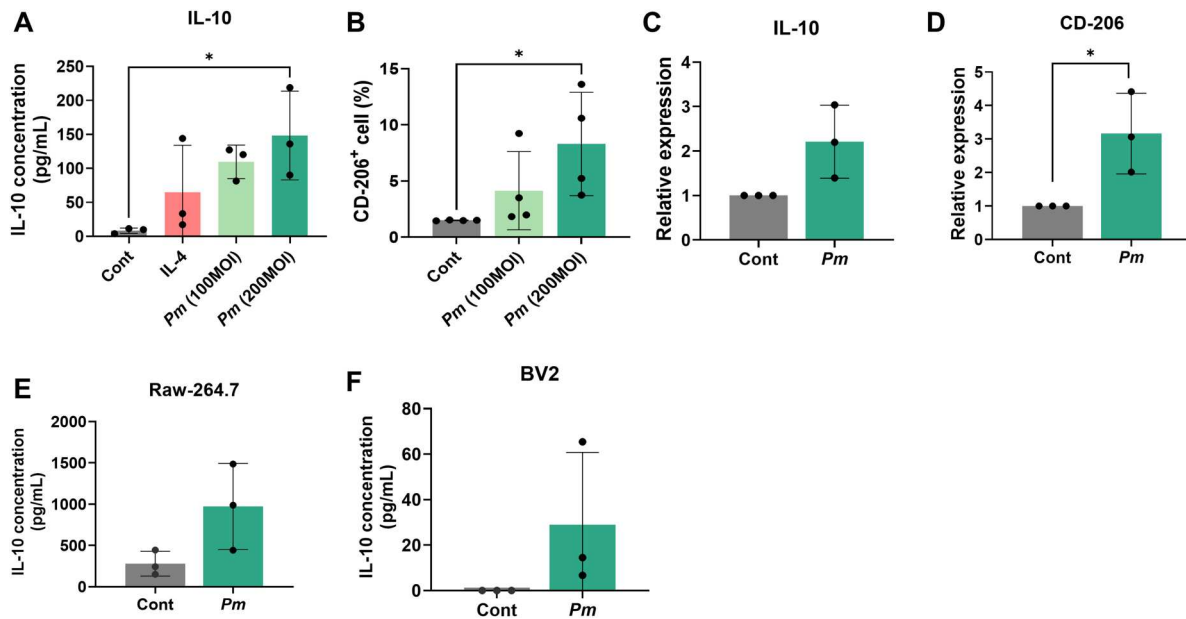


**Figure 2. *Pm* induces the M2-like polarization of macrophages.** (A) ELISA was performed to measure the IL-10 level in the supernatant of THP-1 macrophage cultures with *Pm* (MOIs of 100 and 200) for 24 h or treated with IL-4 (positive control) for 72 h. (B) Flow cytometric analysis was examined for the CD206<sup>+</sup> cells in THP-1 macrophages treated with *Pm* at a MOI of 200 for 24 h. (C and D) qRT-PCR was performed to measure the mRNA level of M2 markers in THP-1 macrophages treated with *Pm* at a MOI of 200 for 24 h. (E and F) ELISA was performed to measure the level of IL-10 in the supernatant of RAW-264.7 and BV-2 treated with *Pm*. All data are displayed as the mean  $\pm$  SD. \* $P < 0.05$ .

(CM) from *Pm*-infected THP-1 cells. We examined the proliferation and cisplatin resistance of CRC cells treated with CM, CM-*Pm*, or normal media (control). CRC cells treated with CM-*Pm* showed significantly increased proliferation (Figure 3(A)) and resistance to cisplatin treatment (Figure 3(B)) compared to those treated with CM or the control. To further validate these findings, we assessed the migratory ability of CRC cells treated with CM-*Pm* using wound healing and transwell assays. CM treatment increased migration in both cell lines, and notably, co-culturing with CM-*Pm* significantly enhanced migratory capability (Figure 3(C)–(F)). In the transwell assay, CM treatment increased the number of stained CRC cells passing through the membrane, and CM-*Pm* further enhanced this effect, indicating an increase in migratory ability (Figure 3(G), (H)). These results suggest that *Pm*-induced M2-like macrophages accelerate the malignant characteristics of CRC cells, emphasizing their role in CRC progression.

### 3.4. Production of pro-inflammatory cytokine IL-8 is elevated in macrophages infected with *Pm*

The influence of EMT on CRC progression, characterized by promoting cell migration, is well-documented (Bhat et al. 2022). Investigating the role of cytokines produced by macrophages in orchestrating EMT and

cancer cell migration is essential for understanding cancer progression. We performed RT-PCR to examine the mRNA levels of cytokines relevant to the EMT and migration of THP-1 macrophages treated with *Pm*. The mRNA levels of several cytokines were elevated in *Pm*-treated cells compared to those in the control. Notably, IL-8 level showed the most significant upregulation among the cytokines (Figure 4(A)). To further confirm this finding, the supernatant of *Pm*-infected THP-1 cells was collected and analyzed using ELISA. Similarly, the level of IL-8 from *Pm*-infected THP-1 cells was significantly increased (Figure 4(B)), suggesting that IL-8 is elevated in *Pm*-treated macrophages.

### 3.5. IL-8 neutralization reverses CM-*Pm*-enhanced migratory properties in CRC cells

Following *Pm* infection, we observed a significant upregulation of IL-8 production in THP-1 cells, suggesting that IL-8 plays a pivotal role in the cellular response to bacterial infection. To directly assess the role of IL-8 in the characteristics of CRC cells, we performed IL-8 neutralization experiments using an anti-IL-8 antibody (IL-8 Ab). HT-29 and HCT-116 cells were cultured in the presence of CM, CM-*Pm*, and CM-*Pm* treated with IL-8 Ab. Consistent with our previous findings, we observed that CM-*Pm* notably increased the migration of CRC

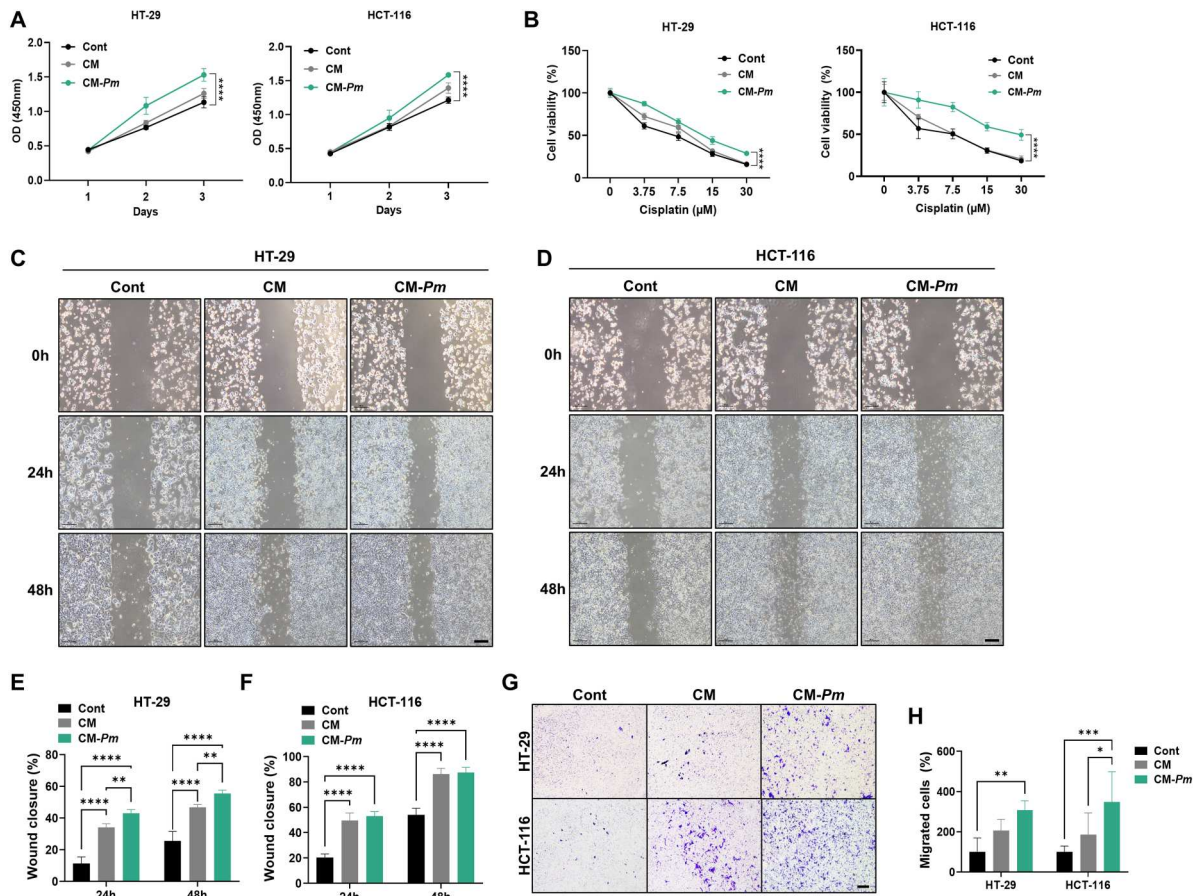


**Figure 3. The conditioned media of macrophages primed with *Pm* facilitates the progression of CRC cells.** (A) CCK8 assay was performed to examine the proliferation of CRC cells in response to CM (conditioned media) and CM-*Pm* (conditioned media with *Pm* infection) from THP-1 macrophages compared to normal media for 24, 48, and 72 h. (B) Cisplatin resistance was examined in CRC cells after 48 h treatment with CM, CM-*Pm*, or control. (C-F) Wound healing assays were conducted, and wound closures (%) were assessed to measure the mobility of CRC cells following 24, 48 h treatment with CM, CM-*Pm*, or control. Scale bar: 100 μm. (G and H) Transwell assay was conducted to examine the migration ability of CRC cells following treatment with CM, CM-*Pm*, or control. All data are displayed as the mean ± SD. \*\* $P < 0.01$ , \*\*\* $P < 0.001$ , and \*\*\*\* $P < 0.0001$ .

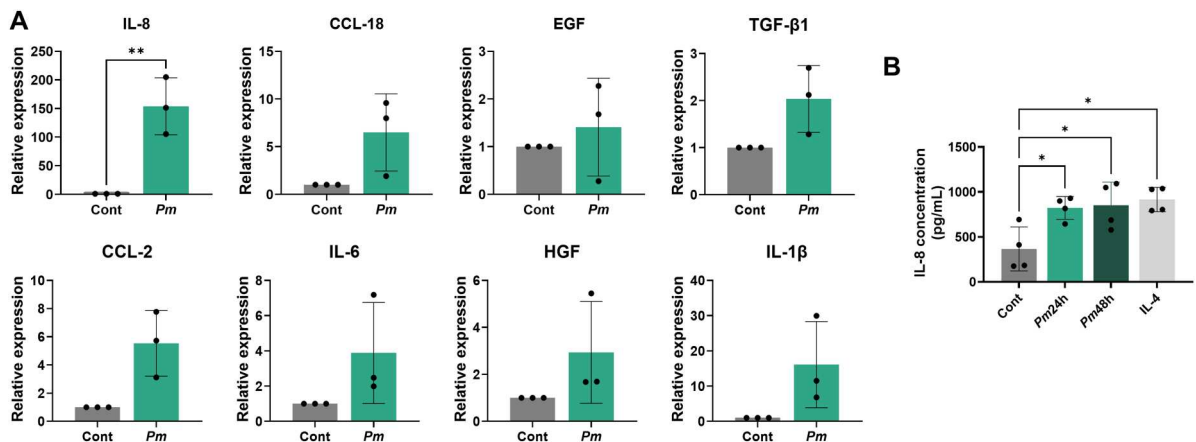


**Figure 4. The production of the pro-inflammatory cytokine IL-8 significantly increases in macrophages treated with *Pm*.** (A) qRT-PCR was conducted to measure the mRNA levels of representative EMT and migration-related cytokines. (B) ELISA was used to analyze the concentration of IL-8 in the supernatant of THP-1 macrophages treated with *Pm* at an MOI of 200 for 24 and 48 h. All data are displayed as the mean ± SD. \* $P < 0.05$  and \*\* $P < 0.01$ .

cells, as confirmed through wound healing assays (Figure 5(A)–(D)). However, the addition of an IL-8 Ab reversed this effect, indicating the pivotal role of IL-8 in mediating this response (Figure 5(A)–(D)). Furthermore, transwell migration assays showed a decrease in the number of stained cells upon IL-8 Ab treatment, indicating reduced migration capabilities induced by CM-*Pm* (Figure 5(E),(F)). These results strongly suggest that IL-8 plays a critical role in enhancing the migratory properties of CRC cells mediated by conditioned media from *Pm*-infected THP-1 cells.

### 3.6. The presence of *Pm* exacerbates the progression of CRC in the AOM/DSS model

To investigate the impact of *Pm* on CRC development, we employed an AOM/DSS-induced mouse model for CRC. Following mutagenesis induction with AOM, mice were exposed to three DSS cycles and received *Pm* or PBS via oral gavage three times weekly (Figure 6(A)). Body weight was monitored at least twice a week, yet no significant weight change was noted between the *Pm* and PBS group (Figure 6(B)). Additionally, diarrhea and rectal bleeding were observed upon DSS exposure. The survival rate in the PBS group was slightly lower

compared to the *Pm* group (Figure 6(C)). No notable difference in colon length was observed between the AOM/DSS-treated mice and the controls (Figure 6(D)). Importantly, all the mice in the AOM/DSS group developed tumors. The *Pm*-treated group not only exhibited a significantly greater tumor count than the PBS group but also showed an increase in tumor mass (Figure 6(E)). Following the collection of colon tissues for analysis, RT-PCR results revealed elevated mRNA levels of CD206 and IL-8 in the colons of mice treated with *Pm* (Figure 6(F)). Taken together, these findings validate that *Pm* is a key factor in accelerating CRC progression.

## 4. Discussion

This study demonstrates that *Pm* plays a significant role in the M2-like polarization of macrophages, potentially influencing the progression of CRC. By modulating macrophage polarization, *Pm* accelerates the aggressive characteristics of CRC cells within the TME. Additionally, our findings highlight that *Pm* exacerbates CRC development in an AOM/DSS-induced colitis-associated cancer model.

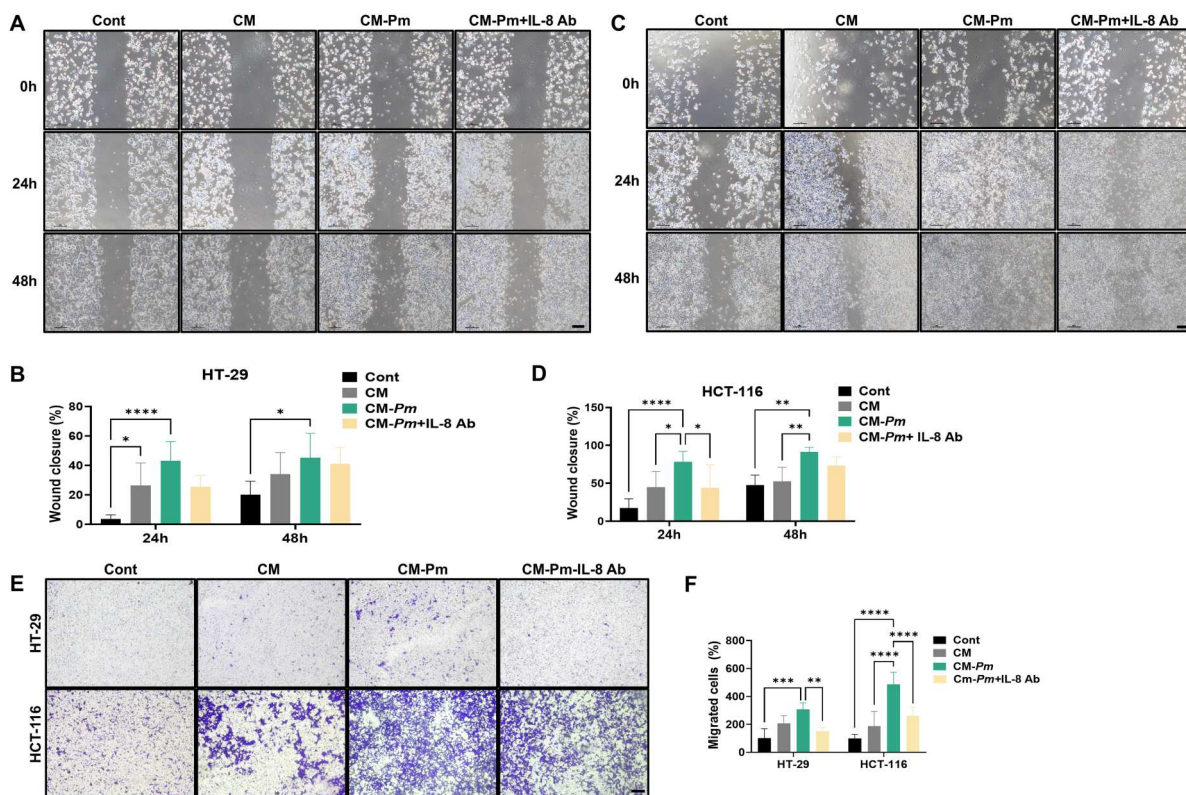


**Figure 5. IL-8 neutralization reverses the effect of CM-*Pm* on inducing migration in CRC cells.** HT-29 and HCT-116 were co-cultured with CM, CM-*Pm*, or CM-*Pm* with IL-8 Ab (500 ng/mL). (A–D) Wound healing assays were conducted to assess the mobility of CRC cells. (E and F) Transwell assay was performed to evaluate the migration of CRC cells. Scale bar: 100  $\mu$ m. All data are displayed as the mean  $\pm$  SD. \* $P < 0.05$ , \*\* $P < 0.01$ , \*\*\* $P < 0.001$  and \*\*\*\* $P < 0.0001$ .



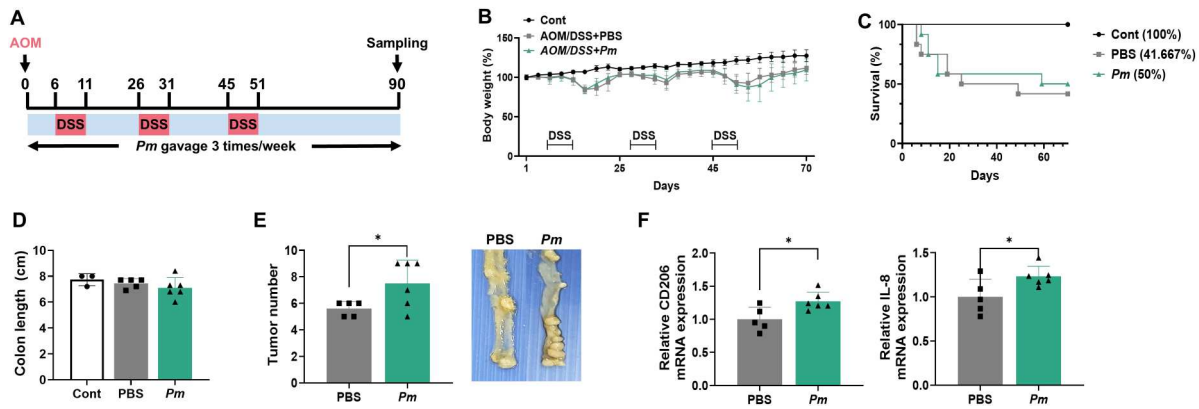


**Figure 6. *Pm* exacerbates the progression of CRC in AOM/DSS model.** (A) A schematic protocol to induce the ulcerative colitis-related colorectal cancer model using AOM/DSS with *Pm* or PBS gavage (Control,  $n = 3$ ; PBS,  $n = 5$ ; *Pm*,  $n = 6$ ). (B) The body weight changes in mice were measured at specific times following AOM administration. (C) The survival rate was calculated on day 70 following euthanization. (D) Colon length was measured in each colon on day 70. (E) Tumor numbers were quantified in each colon, and representative histological images of colon tissues from the PBS and *Pm*-treated groups are shown. (F) qRT-PCR was conducted to assess the mRNA expression levels of CD-206, and IL-8 in colon tissue samples. All data are displayed as the mean  $\pm$  SD.  $*P < 0.05$ .

An increasing body of evidence highlights the association between the prevalence of *Pm* and CRC development, though experimental studies on *Pm* remain scarce. Zhao *et al.* demonstrated a significant increase in HT-29 cell proliferation upon exposure to *Pm*-conditioned media (Zhao *et al.* 2022). Similarly, further research indicated that *Pm* infection enhanced CRC cell proliferation, induced morphological changes, and significantly accelerated wound healing (Hatta *et al.* 2023). In our study, direct treatment with *Pm* modestly increased the proliferation and cisplatin resistance of CRC cells, alongside quicker wound healing. These results imply that *Pm* can influence the characteristics of CRC cells. However, the impact did not align with our initial expectations, as *Pm* failed to significantly alter CRC cell behavior.

Recent studies have suggested that oral pathogens could induce M2-like macrophage polarization, potentially accelerating the progression of CRC. Consequently, *Pm* might impede anti-tumor immunity, advancing CRC progression by modulating immune cells. However, the specificity of *Pm* activation in the immune cells remains elusive. This study explores how *Pm* affects immune cells, discovering that *Pm* leads to the development of M2-like macrophages. Furthermore, the induction of M2-like TAMs by *Pm* significantly enhanced CRC cell proliferation, chemotherapy resistance, and migration. Consistent with prior research, IL-8 secretion, known to facilitate angiogenesis, invasion, and metastasis in several cancers including CRC, was implicated in these processes (Bhat *et al.* 2022; Xiao *et al.* 2018). Heyang *et al.* demonstrated that TAMs secrete cytokines, including IL-6 and IL-8, which promote CRC metastasis (Xu *et al.* 2014). Similarly, Shaza *et al.* found that TAMs

notably secrete IL-8, affecting the invasion and migration of breast cancer cells (Ahmed *et al.* 2021). Aligning with these findings, our study observed a significant increase in IL-8 levels in macrophages following *Pm* treatment, underscoring its potential role in CRC progression. Further investigations are required to fully understand the precise effects of IL-8 on CRC cells.

*F. nucleatum*, a representative oral pathogen, has been reported to induce M2 macrophage polarization and promote CRC progression through activation of the TLR4/NF- $\kappa$ B/S100A9 signaling pathway (Hu *et al.* 2021). TLRs, expressed on various cell types, play a crucial role in the immune response by detecting pathogen-associated molecular patterns (PAMPs) derived from microbial sources (Lim and Staudt 2013). Although TLR4 is typically associated with gram-negative bacteria, it is important to consider that gram-positive bacteria can also modulate TLR-mediated immune responses. For instance, cell wall components of gram-positive bacteria, such as peptidoglycan and lipoteichoic acid, have been shown to activate monocytes and induce immune responses through TLR2 or TLR4 (Schwandner *et al.* 1999; Takeuchi *et al.* 1999). Furthermore, the gram-positive *Propionibacterium acnes* is abundant in gastric cancer tissues and facilitates M2 macrophage polarization via the TLR4/PI3 K/Akt pathway, exacerbating the cancer (Li *et al.* 2021). These observations suggest that *Pm* may also engage TLR4-mediated signaling pathways to induce M2 macrophage polarization, potentially contributing to cancer progression.

Our findings suggest that *Pm*-induced IL-8 secretion plays a critical role in promoting the aggressive behavior of CRC cells. Targeting IL-8 could offer a potential therapeutic approach for CRC treatment. Anti-IL-8 therapies have demonstrated efficacy in stabilizing disease in

patients with advanced solid tumors, including CRC (Bilusic et al. 2019). Furthermore, targeting *Pm* directly, through antibiotic treatment or modulation of the gut microbiome, could mitigate its pro-tumorigenic effects. Further research into the development of diagnostic markers, such as elevated IL-8 or specific microbial signatures may provide early detection methods for CRC patients at higher risk due to *Pm* infection.

Previous studies have elucidated the role of *Pm* in accelerating colorectal tumor development in various mouse models (Chang et al. 2023; Zhao et al. 2022). In this study, the tumor burden in *Pm*-treated mice showed a significantly higher burden, with both an increased number of tumors and greater tumor mass compared to controls, underscoring its tumor-promoting effects.

While these findings provide significant insights, there are several limitations that should be addressed. First, the controlled conditions of our experiments may not fully recapitulate the complexity of CRC development in clinical settings. Additionally, while the AOM/DSS model is widely used to study colitis-associated cancer, it does not entirely reflect the pathogenesis of sporadic CRC in humans. Future studies should consider using additional CRC models to validate these findings. Furthermore, the exact mechanism by which *Pm* interacts with other gut microbiota and its effects on CRC progression remain to be fully elucidated. These limitations highlight the need for further research to fully understand the clinical relevance of *Pm* in CRC.

In conclusion, our study provides new insights into the involvement of *Pm* in the progression of CRC. We suggest that *Pm* infection potentially drives CRC progression by inducing M2-like macrophage polarization, largely via IL-8 secretion. This insight underscores potential therapeutic targets for CRC management.

## Acknowledgments

We would like to thank Editage ([www.editage.co.kr](http://www.editage.co.kr)) for the English language editing.

## Disclosure statement

No potential conflict of interest was reported by the author(s).

## Funding

This study was supported by the National Research Foundation of Korea (NRF), funded by the Ministry of Science and ICT (MSIT) (grant number: 2018-R1A5A2023879, RS-2024-00340037, RS-2024-00347978) and by the Bio & Medical Technology Development Program of NRF funded by the Korean government (MSIT) (grant number: RS-2023-00223591). Korean Fund for Regenerative Medicine (KFRM) grant funded by MSIT and the Ministry of Health & Welfare (grant number: 22A0205L1, 23A0205L1) also supported this project.

## Data availability statement

The data presented in this study are available upon request from the corresponding author.

## References

- Ahmed S, Mohamed HT, El-Husseiny N, Mahdy E, Safwat MM, Diab G, El-Sherif AA, El-Shinawi AA, Mohamed M, M M. 2021. IL-8 secreted by tumor associated macrophages contribute to lapatinib resistance in HER2-positive locally advanced breast cancer via activation of Src/STAT3/ERK1/2-mediated EGFR signaling. *Biochim Biophys Acta Mol Cell Res.* 1868(6):118995. doi:10.1016/j.bbamcr.2021.118995.
- Andriankaja OM, Adatorwovor R, Kantarci A, Hasturk H, Shaddox L, Levine MA. 2023. Periodontal disease, local and systemic inflammation in Puerto Ricans with type 2 diabetes mellitus. *Biomedicines.* 11(10):2770. doi:10.3390/biomedicines11102770.
- Awedew AF, Asefa Z, Belay WB. 2022. Burden and trend of colorectal cancer in 54 countries of Africa 2010-2019: a systematic examination for global burden of disease. *BMC Gastroenterol.* 22(1):204. doi:10.1186/s12876-022-02275-0.
- Bhat AA, Nisar S, Singh M, Ashraf B, Masoodi T, Prasad CP, Sharma A, Maacha S, Karedath T, Hashem S et al. 2022. Cytokine- and chemokine-induced inflammatory colorectal tumor microenvironment: emerging avenue for targeted therapy. *Cancer Commun (Lond).* 42(8):689-715. doi:10.1002/cac2.12295.
- Bilusic M, Heery CR, Collins JM, Donahue RN, Palena C, Madan RA, Karzai F, Marte JL, Strauss J, Gatti-Mays ME et al. 2019. Phase I trial of HuMax-IL8 (BMS-986253), an anti-IL-8 monoclonal antibody, in patients with metastatic or unresectable solid tumors. *J Immunother Cancer.* 7(1):240. doi:10.1186/s40425-019-0706-x.
- Biswas SK, Mantovani A. 2010. Macrophage plasticity and interaction with lymphocyte subsets: cancer as a paradigm. *Nat Immunol.* 11(10):889-896. doi:10.1038/ni.1937.
- Chang Y, Huang Z, Hou F, Liu Y, Wang L, Wang Z, Sun Y, Pan Z, Tan Y, Ding L, et al. 2023. Parvimonas micra activates the Ras/ERK/c-Fos pathway by upregulating miR-218-5p to promote colorectal cancer progression. *J Exp Clin Cancer Res.* 42(1):13. doi:10.1186/s13046-022-02572-2.
- Chen S, Saeed A, Liu Q, Jiang Q, Xu H, Xiao GG, Rao L, Duo Y. 2023. Macrophages in immunoregulation and therapeutics. *Signal Transduct Target Ther.* 8(1):207. doi:10.1038/s41392-023-01452-1.
- Feng J, Read OJ, Dinkova-Kostova AT. 2023. Nrf2 in TIME: The emerging role of nuclear factor erythroid 2-related factor 2 in the tumor immune microenvironment. *Mol Cells.* 46(3):142-152. doi:10.14348/molcells.2023.2183.
- Fong W, Li Q, Yu J. 2020. Gut microbiota modulation: a novel strategy for prevention and treatment of colorectal cancer. *Oncogene.* 39(26):4925-4943. doi:10.1038/s41388-020-1341-1.
- Guo J, Liu H, Guo X, Fang J, Ding T, Zhu H, Cao Y, Xing M, Zheng J, Xu Q, et al. 2021. *Fusobacterium nucleatum* enhances the efficacy of PD-L1 blockade in colorectal cancer. *Signal Transduct Target Ther.* 6(1):398. doi:10.1038/s41392-021-00795-x.
- Hajishengallis G. 2015. Periodontitis: from microbial immune subversion to systemic inflammation. *Nat Rev Immunol.* 15(1):30-44. doi:10.1038/nri3785.

- Hao NB, Lu MH, Fan YH, Cao YL, Zhang ZR, Yang SM. 2012. Macrophages in tumor microenvironments and the progression of tumors. *Clin Dev Immunol.* 2012:948098.
- Hatta MNA, Hanif M, Chin EA, Low SF, Neoh TY, M H. 2023. *Parvimonas micra* infection enhances proliferation, wound healing, and inflammation of a colorectal cancer cell line. *Biosci Rep.* 43(6):BSR20230609. doi:10.1042/BSR20230609.
- Hou K, Wu Z-X, Chen X-Y, Wang J-Q, Zhang D, Xiao C, Zhu D, Koya JB, Wei L, Li J, Chen Z-S. 2022. Microbiota in health and diseases. *Signal Transduct Target Ther.* 7(1):135. doi:10.1038/s41392-022-00974-4.
- Hourani T, Holden JA, Li W, Lenzo JC, Hadjigol S, O'Brien-Simpson NM. 2021. Tumor associated macrophages: origin, recruitment, phenotypic diversity, and targeting. *Front Oncol.* 11:788365. doi:10.3389/fonc.2021.788365.
- Hu L, Liu Y, Kong X, Wu R, Peng Q, Zhang Y, Zhou L, Duan L. 2021. *Fusobacterium nucleatum* facilitates M2 macrophage polarization and colorectal carcinoma progression by activating TLR4/NF-kappaB/S100A9 cascade. *Front Immunol.* 12:658681. doi:10.3389/fimmu.2021.658681.
- Idrissi Janati A, Karp I, Latulippe JF, Charlebois P, Emami E. 2022. Periodontal disease as a risk factor for sporadic colorectal cancer: results from COLDENT study. *Cancer Causes Control.* 33(3):463–472. doi:10.1007/s10552-021-01541-y.
- Kim B, Park YY, Lee JH. 2024. CXCL10 promotes melanoma angiogenesis and tumor growth. *Anim Cells Syst (Seoul).* 28(1):453–465. doi:10.1080/19768354.2024.2402024.
- Kim J, Lee HK. 2021. Potential role of the Gut microbiome in colorectal cancer progression. *Front Immunol.* 12:807648. doi:10.3389/fimmu.2021.807648.
- Kim SW, Kim CW, Moon YA, Kim HS. 2024. Reprogramming of tumor-associated macrophages by metabolites generated from tumor microenvironment. *Anim Cells Syst (Seoul).* 28(1):123–136. doi:10.1080/19768354.2024.2336249.
- Koveitypour Z, Panahi F, Vakilian M, Peymani M, Seyed Forootan F, Nasr Esfahani MH, Ghaedi K. 2019. Signaling pathways involved in colorectal cancer progression. *Cell Biosci.* 9:97. doi:10.1186/s13578-019-0361-4.
- Lee H, Park SJ, Hong S, Lim SW, Kim S. 2022. Deletion of IP6K1 in mice accelerates tumor growth by dysregulating the tumor-immune microenvironment. *Anim Cells Syst (Seoul).* 26(1):19–27. doi:10.1080/19768354.2022.2029560.
- Li Q, Wu W, Gong D, Shang R, Wang J, Yu H. 2021. *Propionibacterium acnes* overabundance in gastric cancer promote M2 polarization of macrophages via a TLR4/PI3 K/Akt signaling. *Gastric Cancer.* 24(6):1242–1253. doi:10.1007/s10120-021-01202-8.
- Lim KH, Staudt LM. 2013. Toll-like receptor signaling. *Cold Spring Harb Perspect Biol.* 5(1):a011247.
- Liu Y, Lau HC, Cheng WY, Yu J. 2023. Gut microbiome in colorectal cancer: clinical diagnosis and treatment. *Genomics Proteomics Bioinformatics.* 21(1):84–96. doi:10.1016/j.gpb.2022.07.002.
- Lowenmark T, Li X, Lofgren-Burstrom A, Zingmark C, Ling A, Kellgren TG, Larsson P, Ljuslinder I, Wai SN, Edin S, et al. 2022. *Parvimonas micra* is associated with tumour immune profiles in molecular subtypes of colorectal cancer. *Cancer Immunol Immunother.* 71(10):2565–2575. doi:10.1007/s00262-022-03179-4.
- Mohammadi M, Mirzaei H, Motallebi M. 2022. The role of anaerobic bacteria in the development and prevention of colorectal cancer: A review study. *Anaerobe.* 73:102501. doi:10.1016/j.anaerobe.2021.102501.
- Nguyen HT, Duong HQ. 2018. The molecular characteristics of colorectal cancer: implications for diagnosis and therapy. *Oncol Lett.* 16(1):9–18.
- Osman MA, Neoh HM, Ab Mutalib NS, Chin SF, Mazlan L, Raja Ali RA, Zakaria AD, Ngiu CS, Ang MY, Jamal R. 2021. *Parvimonas micra*, *peptostreptococcus stomatis*, *fusobacterium nucleatum* and *Akkermansia muciniphila* as a four-bacteria biomarker panel of colorectal cancer. *Sci Rep.* 11(1):2925. doi:10.1038/s41598-021-82465-0.
- Pan Y, Yu Y, Wang X, Zhang T. 2021. Corrigendum: tumor-associated macrophages in tumor immunity. *Front Immunol.* 12:775758. doi:10.3389/fimmu.2021.775758.
- Perez-Gonzalez A, Bevant K, Blanpain C. 2023. Cancer cell plasticity during tumor progression, metastasis and response to therapy. *Nat Cancer.* 4(8):1063–1082. doi:10.1038/s43018-023-00595-y.
- Purcell RV, Visnovska M, Biggs PJ, Schmeier S, Frizelle FA. 2017. Distinct gut microbiome patterns associate with consensus molecular subtypes of colorectal cancer. *Sci Rep.* 7(1):11590. doi:10.1038/s41598-017-11237-6.
- Rawla P, Sunkara T, Barsouk A. 2019. Epidemiology of colorectal cancer: incidence, mortality, survival, and risk factors. *Prz Gastroenterol.* 14(2):89–103.
- Schwandner R, Dziarski R, Wesche H, Rothe M, Kirschning CJ. 1999. Peptidoglycan- and lipoteichoic acid-induced cell activation is mediated by toll-like receptor 2. *J Biol Chem.* 274(25):17406–17409. doi:10.1074/jbc.274.25.17406.
- Stoffel EM, Murphy CC. 2020. Epidemiology and mechanisms of the increasing incidence of colon and rectal cancers in young adults. *Gastroenterology.* 158(2):341–353. doi:10.1053/j.gastro.2019.07.055.
- Takeuchi O, Hoshino K, Kawai T, Sanjo H, Takada H, Ogawa T, Takeda K, Akira S. 1999. Differential roles of TLR2 and TLR4 in recognition of gram-negative and gram-positive bacterial cell wall components. *Immunity.* 11(4):443–451. doi:10.1016/S1074-7613(00)80119-3.
- Xiao P, Long X, Zhang L, Ye Y, Guo J, Liu P, Zhang R, Ning J, Yu W, Wei F, et al. 2018. Neurotensin/IL-8 pathway orchestrates local inflammatory response and tumor invasion by inducing M2 polarization of tumor-associated macrophages and epithelial-mesenchymal transition of hepatocellular carcinoma cells. *Oncoimmunology.* 7(7):e1440166. doi:10.1080/2162402X.2018.1440166.
- Xu Chaochao, Fan Lina, Lin Yifeng, Shen Weiyi, Qi Yadong, Zhang Ying, Chen Zhehang, Wang Lan, Long Yanqin, Hou Tongyao, et al. 2021. *Fusobacterium nucleatum* promotes colorectal cancer metastasis through miR-1322/CCL20 axis and M2 polarization. *Gut Microbes.* 13(1). doi:10.1080/19490976.2021.1980347.
- Xu H, Lai W, Zhang Y, Liu L, Luo X, Zeng Y, Wu H, Lan Q, Chu Z. 2014. Tumor-associated macrophage-derived IL-6 and IL-8 enhance invasive activity of LoVo cells induced by PRL-3 in a KCNN4 channel-dependent manner. *BMC Cancer.* 14:330. doi:10.1186/1471-2407-14-330.
- Zhao L, Zhang X, Zhou Y, Fu K, Lau HC, Chun TW, Cheung AH, Coker OO, Wei H, Wu WK, et al. 2022. *Parvimonas micra* promotes colorectal tumorigenesis and is associated with prognosis of colorectal cancer patients. *Oncogene.* 41(36):4200–4210. doi:10.1038/s41388-022-02395-7.